Cross-neutralization of SARS-CoV-2 by HIV-1 specific broadly neutralizing antibodies and polyclonal plasma

Nitesh Mishra[1], Sanjeev Kumar[1,2], Swarandeep Singh[1], Tanu Bansal[1], Nishkarsh Jain[1], Sumedha Saluja[1], Jayanth Kumar Palanichamy[1], Riyaz A. Mir[1], Subrata Sinha[1], Kalpana Luthra[1*].

[1]Department of Biochemistry, All India Institute of Medical Sciences, New Delhi, India – 110029.

[2]Current address – ICGEB-Emory Vaccine Centre, International Centre for Genetic Engineering and Biotechnology, New Delhi - 110067, India.

*Correspondence – Kalpana Luthra (kalpanaluthra@gmail.com)

Abstract

Cross-reactive epitopes (CREs) are similar epitopes on viruses that are recognized or neutralized by same antibodies. The S protein of SARS-CoV-2, similar to type I fusion proteins of viruses such as HIV-1 envelope (Env) and influenza hemagglutinin, is heavily glycosylated. Viral Env glycans, though host derived, are distinctly processed and thereby recognized or accommodated during antibody responses. In recent years, highly potent and/or broadly neutralizing human monoclonal antibodies (bnAbs) that are generated in chronic HIV-1 infections have been defined. These bnAbs exhibit atypical features such as extensive somatic hypermutations, long complementary determining region (CDR) lengths, tyrosine sulfation and presence of insertions/deletions, enabling them to effectively neutralize diverse HIV-1 viruses despite extensive variations within the core epitopes they recognize. As some of the HIV-1 bnAbs have evolved to recognize the dense viral glycans and cross-reactive epitopes (CREs), we assessed if these bnAbs cross-react with SARS-CoV-2. Several HIV-1 bnAbs showed cross-reactivity with SARS-CoV-2 while one HIV-1 CD4 binding site bnAb, N6, neutralized SARS-CoV-2. Furthermore, neutralizing plasma antibodies of chronically HIV-1 infected children showed cross neutralizing activity against SARS-CoV-2. Collectively, our observations suggest that human monoclonal antibodies tolerating extensive epitope variability can be leveraged to neutralize pathogens with related antigenic profile.

Importance

In the current ongoing COVID-19 pandemic, neutralizing antibodies have been shown to be a critical feature of recovered patients. HIV-1 bnAbs recognize extensively diverse cross-reactive epitopes and tolerate diversity within their core epitope. Given the unique nature of HIV-1 bnAbs and their ability to recognize and/or accommodate viral glycans, we reasoned that the glycan shield of SARS-CoV-2 spike protein can be targeted by HIV-1 specific bnAbs. Herein, we showed that HIV-1 specific antibodies cross-react and neutralize SARS-CoV-2. Understanding cross-reactive neutralization epitopes of antibodies generated in divergent viral infections will provide key evidence for engineering so called super-antibodies (antibodies that can potently neutralize diverse pathogens with similar antigenic features). Such cross-reactive antibodies can provide a blueprint upon which synthetic variants can be generated in the face of future pandemics.

Introduction

Broadly neutralizing antibodies (bnAbs) targeting the HIV-1 envelope glycoprotein (Env) can neutralize a broad range of circulating HIV-1 isolates and have been called super-antibodies due to their remarkable potency and neutralization breadth (1). As a result of its extensive genetic diversity, HIV-1 is subdivided in multiple clades and circulating recombinant forms (CRFs). A rare subset of HIV-1 infected individuals develops broad and potent antibody responses and have served as potential candidates for the isolation of HIV-1 bnAbs (2, 3). HIV-1 bnAbs take years to develop, have atypical features including long complementarity-determining regions (CDR) loops, high levels of somatic hypermutations (SHMs), presence of insertions and/or deletions (indels), tyrosine sulfation, and develop to tolerate significant alterations in their core epitope (1–3). Notably, V2-apex bnAbs have been shown to exhibit cross-group neutralization activity with viruses derived from HIV-1 group M, N, O and P Envs. Furthermore, they even show cross-neutralization of simian immunodeficiency virus (SIV) isolates (4).

Severe acute respiratory syndrome coronavirus 2 (SARS-CoV-2) emerged in late 2019, rapidly spread across different countries, infecting millions of individuals and has caused a global COVID-19 pandemic (5). The SARS-CoV-2 trimeric spike glycoprotein (S) binds to angiotensin-converting enzyme 2 (ACE2) which leads to host cell entry and fusion (6, 7). Type 1 viral fusion machines, including HIV-1 Env, Influenza hemagglutinin (HA), and SARS-CoV-2 S protein, mediate viral entry driven by structural rearrangements and are trimeric in their pre-fusion and post-fusion state (2, 7, 8). SARS-CoV-2 S protein is covered by host-derived glycans on 66 PNGS on each trimer and site-specific glycan analysis has shown that 28% of glycans on the protein surface are underprocessed oligomannose-type glycans (9). SARS-CoV and HCoV OC43 elicited antibodies have been shown to cross-react with SARS-CoV-2. The Neutralizing antibody (nAb), S309, isolated from memory B-cells of a SARS-CoV infected individual targets a glycan epitope conserved within the Sarbecovirus subgenus (10). Several HIV-1 bnAbs have been shown to penetrate the glycan shield and contact protein residues in Env via their long complementary determining region (CDR) loops and make stabilizing contacts with the surrounding high mannose and complex glycans (11, 12). Several HIV-1 bnAbs recognize glycopeptides and/or cluster of N-linked glycans (1–3). The glycans on HIV-1 Env are highly dynamic and can be occupied by different glycoforms due to glycan processing. The glycan shield covering the HIV-1 Env comprises roughly half its mass and shields approximately 70% of the protein surface with glycosylation occurring on potential N-linked glycosylation sites that vary significantly between infected individuals (18 – 33 PNGS) (13, 14).

Herein, we reasoned that given the unique nature of HIV-1 bnAbs and their ability to recognize and/or accommodate viral glycans, the glycan shield of SARS-CoV-2 spike protein can be targeted by HIV-1 specific bnAbs.

Results and Discussion

In the past decade, a large panel of bnAbs and non-nAbs targeting diverse epitopes on the HIV-1 Env glycoprotein have been isolated and extensively characterized (reviewed in refs (1–3)). To evaluate the potential cross-reactivity of these antibodies, we first performed binding ELISA of 30 bnAbs and 7 non-

nAbs with SARS-CoV-2 $S2P_{ecto}$ protein (pre-fusion stabilized ectodomain construct, 1 – 1208 amino acid residues) and receptor-binding domain (RBD, residues 319 – 541, also called $S1^B$ domain). The HIV-1 bnAbs were categorized into five categories based on their epitopes on the viral Env (**figure 1A)**. CR3022, a nAb isolated from a convalescent SARS-CoV patient (15), which has been shown to cross-react with SARS-CoV-2 (7), was used as positive control while two antibodies targeting the envelope glycoprotein of simian immunodeficiency virus were used as negative control. Of the 30 HIV-1 bnAbs tested for binding to both $S2P_{ecto}$ protein and RBD of SARS-CoV-2, 6 bnAbs (VRC07.523LS, NIH45-46 G54W, N6, Z13e1, 2F5 and 4E10) showed significant binding, while one bnAb (CAP256.09) showed moderate binding to only the $S2P_{ecto}$ protein (**figure 1A**). Non-nAbs that target post-fusion and/or open trimeric conformation of HIV-1 Env were unable to bind both SARS-CoV-2 $S2P_{ecto}$ protein and RBD protein (**figure 1B**), suggesting that only pre-fusion state specific antibodies that evolve via extensive somatic hypermutation and affinity maturation in response to repeated exposure to a continuously evolving antigen can cross react with other viruses.

A

bnAb	HIV-1 epitope class	RBD	S2P
PG9	V2-Apex	0.92	3.85
PG16		0.61	1.23
PGT145		1.14	1.54
PGDM1400		0.65	1.08
CAP256.09		3.05	7.04
CAP256.25		1.09	2.33
CH01		1.13	1.96
10-1074	V3-Glycan	1.77	2.88
BG18		0.73	0.91
AIIMS-P01		1.12	1.41
PGT121		1.49	2.26
PGT126		1.65	1.91
PGT128		1.61	1.48
PGT135		0.82	0.78
2G12		0.85	1.21
VRC01	CD4-binding-site	1.03	2.02
VRC03		0.65	1.69
VRC07.523LS		16.12	20.48
N6		26.23	23.21
3BNC117		0.96	2.01
VRC-CH31		0.82	1.01
CH106		1.97	2.97
NIH45-46 G54W		17.54	14.04
PGT151	Interface	1.15	2.07
35O22		1.86	2.23
VRC34.01		1.09	0.91
10E8	MPER	0.72	1.59
Z13e1		30.76	24.87
4E10		33.45	25.81
2F5		21.02	18.73
CR3022	Positive	36.71	34.83
KK15	Negative	0.59	0.61
KK45		0.61	0.91

B

mAb	HIV-1 epitope class	RBD	S2P
240D	non-nAbs	1.61	1.74
447-52d		0.99	0.91
48d		0.89	0.71
A32		0.88	0.84
39F		0.95	0.81
17b		0.84	0.94
b6		0.63	0.57

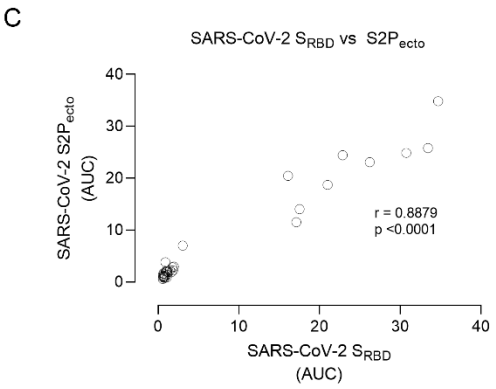

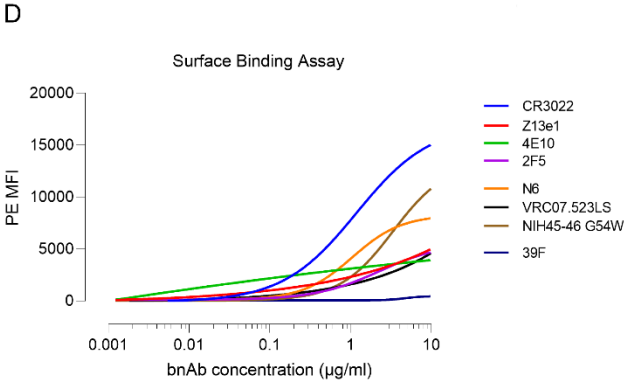

Figure 1 – HIV-1 bnAbs cross-react with the receptor binding domain of SARS-CoV-2. (A – B) Cross-reactivity of anti-HIV-1 broadly neutralizing antibodies targeting diverse epitopes on HIV-1 Env and non-neutralizing

antibodies were assessed by ELISA using SARS-CoV-2_{RBD} and SARS-CoV-2 $S2P_{ecto}$. CR3022, a SARS-CoV neutralizing antibody, was used as positive control. Two antibodies targeting SIV Env were used as negative control. Area under curve (AUC) of OD_{450} values of a 12-point binding curve (range, 0.0048 to 10 µg/ml) from three independent experiments are shown. (C) Two-tailed Spearman's correlation was calculated using the area under curve (AUC) values. A significant positive correlation was observed between RBD and $S2P_{ecto}$ (spearman r = 0.8879, p <0.0001). (D) Binding of HIV-1 bnAbs that showed cross-reactivity to S2P and RBD domain of SARS-CoV-2 in ELISA to full-length SARS-CoV-2 S glycoprotein expressed on the surface of HEK293T cells. Average median fluorescence intensity values of a 12-point binding curve (range, 0.0048 to 10 µg/ml) from three independent experiments were used to draw the curve. CR3022, a SARS-CoV neutralizing antibody, was used as positive control.

Though reactivity against RBD was stronger than $S2P_{ecto}$ protein for majority of the bnAbs tested, a significant positive correlation was seen between binding to $S2P_{ecto}$ protein and RBD (**Figure 1C**). All the 6 bnAbs that showed binding reactivity in ELISA exhibited a similar binding profile to the cell surface expressed SARS-CoV-2 S glycoprotein (**figure 1D**). Of the 30 monoclonal antibodies tested herein, bnAbs targeting the membrane proximal external region (MPER) of HIV-1 showed maximum binding to both the S protein and RBD with half-maximal effective concentration (EC_{50}) of 0.71 µg/ml and 1.71 µg/ml (Z13e1), 0.048 µg/ml and 2.91 µg/ml (2F5) and 0.79 and 0.33 µg/ml (4E10) µg/ml to the RBD and $S2P_{ecto}$ respectively. VRC07.523LS is an engineered variant of the VRC01 bnAb with higher SHM (16) and while it showed binding to both $S2P_{ecto}$ protein and RBD, both VRC01 and its somatic related clone VRC03 did not show any binding (**figure 2A – B**).

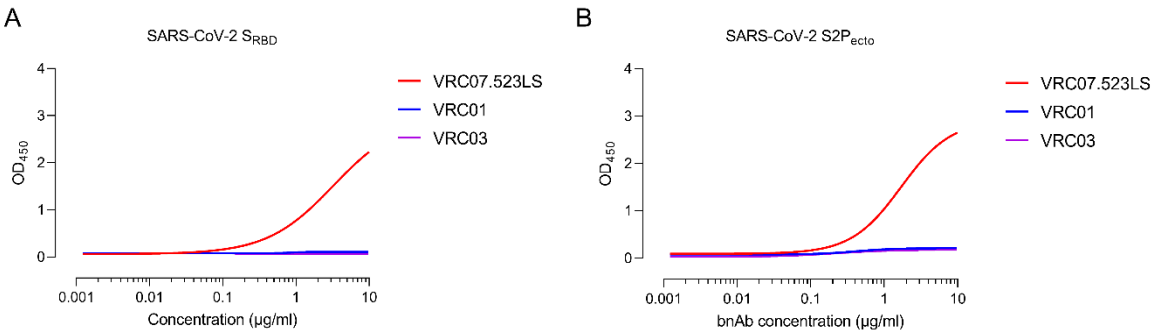

Figure 2 – Somatically engineered VRC07.523LS cross-reacts with SARS-CoV-2. Cross-reactivity of anti-HIV-1 broadly neutralizing antibodies, VRC07.523LS, VRC01 and VRC03, targeting the CD4-binding site on HIV-1 Env. Cross-reactivity was assessed by ELISA using (a) SARS-CoV-2_{RBD} and (b) SARS-CoV-2 $S2P_{ecto}$. OD_{450}, optical density at 450 nm. OD_{450} values are from a 12-point binding curve (range, 0.0048 to 10 µg/ml).

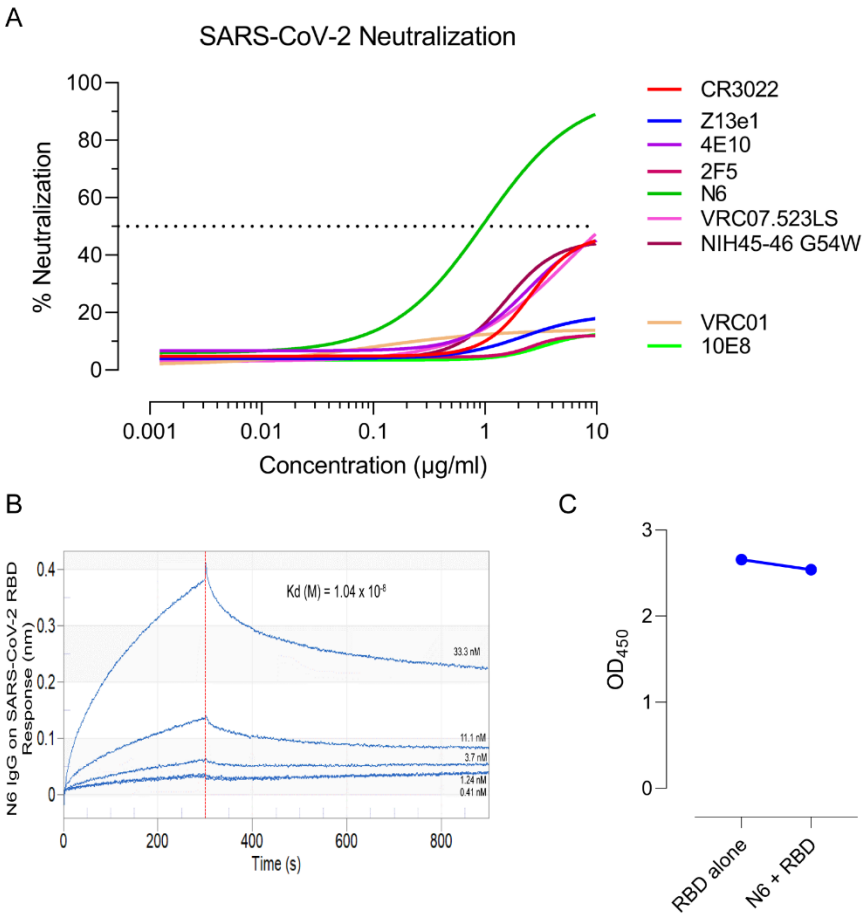

Figure 3 – Neutralization of SARS-CoV-2 by HIV-1 bnAbs. (A) **The** bnAbs were tested for neutralization of pseudotyped SARS-CoV-2 virions. Percent neutralization was calculated by assessing relative luminescence units (RLU) in cell lysates of HEK293T-ACE2 cells 48 hours after infection with SARS-CoV-2 pseudoviruses in the presence of increasing amounts of bnAbs (range, 0.0048 to 10 µg/ml). N6, an anti-HIV-1 CD4-binding site bnAb, showed cross-neutralization of SARS-CoV-2. Dotted line corresponds to 50% neutralization. Graphs were plotted using average values (percent neutralization) from three independent experiments. (B) Affinity of N6 against SARS-CoV-2 RBD was measured using biolayer interferometry. (C) Competition ELISA was performed for RBD binding to ACE2 in presence and absence of N6. Average OD_{450} value from three independent experiments are shown.

All 6 HIV-1 bnAbs that showed binding to SARS-CoV-2 S protein and RBD were then tested for their ability to block infection using a HIV-1 pseudovirus based neutralization assay utilizing SARS-CoV-2 spike protein. VSV-G and MLV pseudotyped viruses were used as negative control. Except N6, all remaining five bnAbs failed to neutralize SARS-CoV-2 (**figure 3A**). Though N6 showed neutralization of SARS-CoV-2, it failed to show complete neutralization (maximum percent neutralization of 88% with an IC_{50} of 0.988 µg/ml) and had a moderate affinity of 1.04 x 10^{8} M (**figure 3B**). Furthermore, N6 failed to block RBD binding to soluble ACE2 by ELISA (**figure 3C**), suggesting it recognizes an epitope on RBD outside the ACE2 binding site. It is noteworthy that N6 is a member of the VRC01 class of antibodies that target the CD4bs of HIV-1; it recognizes HIV-1 in an unusual orientation and neutralizes HIV-1 isolates that are typically resistant to other VRC01 class bnAbs (17). Furthermore, it can tolerate absence of key CD4bs antibody contact residues across the length of heavy chain and can tolerate escape mutations that typically provide resistance to HIV-1 from other CD4bs bnAbs. Of note, N6 has an unprecedented degree of somatic hypermutation (31% in heavy and 25% in light chain at the nucleotide level).

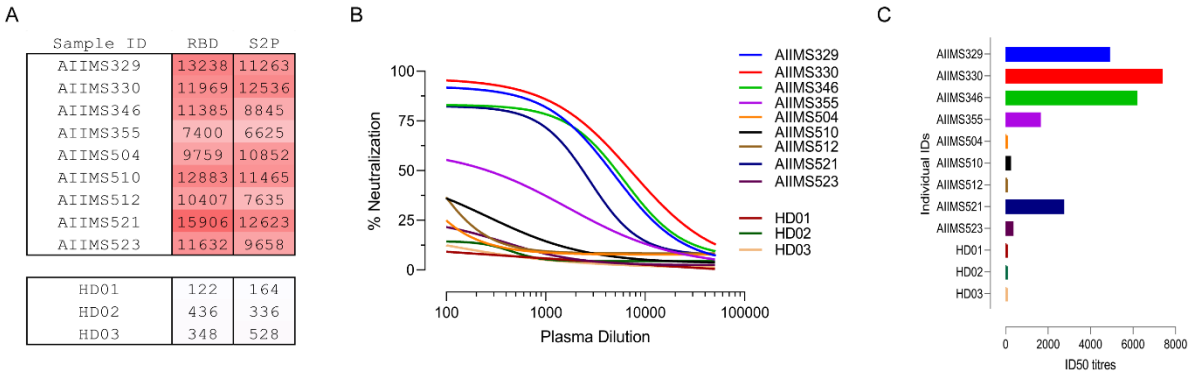

Figure 4 – Polyclonal plasma of HIV-1 infected children neutralizes SARS-CoV-2. (A) Cross-reactivity of anti-HIV-1 neutralizing plasma antibodies from ten children with chronic HIV-1 infection against SARS-CoV-2_{RBD} and SARS-CoV-2 $S2P_{ecto}$ was assessed by ELISA. Plasma antibodies from three seronegative healthy donors were used as negative control. Area under the curve (AUC) of OD_{450} values of a 12-point binding curve (range, inverse plasma dilution of 100 to 51200), from three independent experiments are shown. (B) Plasma samples were tested for their neutralization of pseudotyped SARS-CoV-2 virions. Percent neutralization was calculated by assessing relative luminescence units (RLU) in cell lysates of HEK293T-ACE2 cells 48 hours after infection with SARS-CoV-2 pseudoviruses in the presence of increasing dilution of plasma samples (range, inverse plasma dilution of 100 to 51200). (C) Respective ID_{50} (50% inhibitory dilution) for plasma from all ten children are shown.

We next tested plasma antibodies of children with chronic HIV-1 infection for their ability to bind SARS-CoV-2 $S2P_{ecto}$ protein and RBD. Ten children that had shown potent neutralization titre against a 12-virus global panel of HIV-1 isolates from previous studies in our lab were selected (18–20). While all ten children showed significant binding to both $S2P_{ecto}$ and RBD (**figure 4A**), three children showed potent and near-complete neutralization of SARS-CoV-2 pseudoviruses (AIIMS329, AIIMS330, AIIMS346) while two children (AIIMS355 and AIIMS521) showed moderate neutralization of SARS-CoV-2 (**figure 4B – C**). Collectively, our findings highlight the ability of HIV-1 specific bnAbs and polyclonal plasma to cross-react with the newly emerged SARS-CoV-2.

Neutralizing antibodies engage the host immune system to clear the pathogen or infected cells and are promising candidates for combating emerging viruses (21–23). The RBD of coronaviruses are highly immunogenic and infected individuals typically mount a nAb response (10, 24–28). Given that several HIV-1 bnAbs showed cross-reactivity with RBD of both SARS-CoV and SARS-CoV-2, vaccine efforts should focus inducing antibodies targeting the cross-reactive epitopes on RBD. Most HIV-1 vaccine candidates are in the stage where they typically induce tier 1B or 2 responses against autologous and heterologous viruses in rabbits and non-human primates (29–31). A germline targeting HIV-1 candidate immunogen (eOD-GT8) which was designed to prime VRC01 class CD4bs directed antibodies has been described and the frequencies and affinity of B cells from healthy HIV-1 uninfected individuals recognizing this germline-targeting immunogen showed its suitability as a candidate human vaccine prime (32, 33). Naive B-cells that recognised eOD-GT8 had L-CDR3 sequences that matched several VRC01 class bnAbs, suggesting B-cells with light chain sequences for VRC01 class exist at high frequency. Based on the above observations and the availability of sera from these immunized animals, and findings herein of the ability of HIV-1 CD4bs directed bnAbs to inhibit SARS-CoV and SARS-CoV-2 pseudovirus infection, it is pertinent that the immune sera be tested for binding and neutralization of SARS-CoV-2. Furthermore, detailed structural studies should be taken with N6 to identify its epitope

and neutralization determinants, which can be used to engineer its variants as effective SARS-CoV-2 therapeutics.

Understanding cross-reactive neutralization epitopes of antibodies generated in divergent viral infections can provide key evidence for engineering so called super-antibodies (antibodies that can potently neutralize diverse pathogens with similar antigenic features). Such cross-reactive antibodies can provide a blueprint upon which synthetic variants can be generated in the face of future pandemics.

Methods

Study design

The current study was designed to assess the cross-reactivity of HIV-1 broadly neutralizing antibodies and plasma antibodies from children with chronic HIV-1 infection against the SARS-CoV-2. The study was approved by the institute ethics committee of All India Institute of Medical Sciences (IEC/NP-295/2011 & IEC/59/08.01.16).

Cell lines

HEK293T cells for pseudovirus production and generation of 293T-ACE2 cells, and TZM-bl cells for HIV-1 pseudovirus neutralization assay were maintained at 37^{o}C in 5% CO_2 DMEM containing 10% heat-inactivated FBS (vol/vol), 10mM HEPES, 1mM sodium pyruvate, and 100 U ml^{-1} penicillin/streptomycin. Expi293F cells for recombinant antigen and monoclonal antibody production (Thermo Fisher Scientific, A1452) were maintained at 37^{o}C in 8% CO_2 in Expi293F expression medium (Thermo Fisher Scientific, A1435102).

Plasmids

phCMV3 expression plasmids encoding the soluble S2P ectodomain of SARS-CoV (residue 1 – 1190), SARS-CoV-2 (residue 1 – 1208), RBD domain of SARS-CoV (residue 319 – 513) and SARS-CoV-2 RBD (residue 332 – 527) were kindly gifted by Dr. Raiees Andrabi (The Scripps Research Institute). pCR3 expression vectors encoding truncated version of SARS-CoV S protein (residue 1 – 1236) and SARS-CoV-2 S protein (residue 1 – 1254), and pNL4-3ΔEnv-nanoluc were kindly gifted Dr. Paul Bieniasz (The Rockefeller University). CR3022 fab heavy (GenBank: DQ168569.1) and light (GenBank: DQ168570.1) chains were synthesized commercially and subcloned in phCMV3.

Bacteria

E. coli DH5α, DH10β and STBL3 for propagation of plasmids were cultured at 37^{o}C (30^{o}C for STBL3) in LB broth (Sigma-Aldrich) with shaking at 220 rpm.

Plasma from children with chronic HIV-1 infection

Well-characterized plasma sample from ten children that had shown potent neutralization titre against a 12-virus global panel of HIV-1 isolates from previous studies in our lab were selected.

Recombinant protein production and purification

SARS-CoV and SARS-CoV-2 ectodomain and RBD constructs were transiently transfected in Expi293F cells at a density of 2 million cells/mL using polyethylenimine and expression plasmids at a molar ratio of 3:1 and purified from clarified transfected culture supernatants 4-days post-transfection using Ni^{2+}-NTA affinity chromatography (GE Life Sciences). Proteins were eluted from the column using 250 mmol/L imidazole, dialyzed into phosphate buffered saline (PBS), pH 7.2 and concentrated using Amicon 10-kDa (RBD) and 100-kDa ($S2P_{ecto}$) Amicon ultra-15 centrifugal filter units (EMD Millipore). Protein concentration was determined by the Nanodrop method using the protein molecular weight and molar extinction coefficient as determined by the online ExPASy software (ProtParam).

Antibody production and purification

The HIV-1 monoclonal antibodies (PGT145, CAP256.25, VRC01, 10-1074, BG18, AIIMS-P01, and PGT151) were expressed by co-transfection of heavy chain and light chain IgG1 plasmids (1:1 molar ratio) in Expi293F cells at a density of 0.8 – 1.2 million cells/mL using PEI-Max (1:3 molar ratio) as the transfection reagent. Five days post-transfection, antibodies were purified from clarified supernatants using protein A beads, eluted with IgG elution buffer and concentrated using 10-kDa Amicon ultra-15 centrifugal filter units (EMD Millipore).

Binding ELISA

96-well microtiter plates were coated overnight with 2 µg/ml of purified SARS-CoV $S2P_{ecro}$, SARS-CoV-2 $S2P_{ecto}$, SARS-CoV RBD and SARS-CoV-2 RBD. Plates were blocked with 1% BSA for 3 hours. Monoclonal antibodies were added at a starting concentration of 10 µg/ml, with 11-point titration, and incubated for 2 hours at room temperature. Horseradish peroxidase conjugated goat anti-human IgG was used as secondary antibody and TMB substrate was used for color development. Absorbance at 450 nm was measured using a spectrophotometer.

Generation of 293T-ACE2 cells

VSV-G pseudotyped lentiviruses packaging the human ACE2 were generated by co-transfecting the HEK293T cells with pHAGE6-CMV-ACE2-ZsGreen plasmid and lentiviral helper plasmids (HDM-VSV-G, HDM-Hgpm2, HDM-Tat and CMV-Rev). 48 hours post-transfection, lentiviruses were harvested and used to infect HEK293T cells pre-seeded 24-hours in the presence of 10 µg/ml polybrene. 3-days post-infection, transduced cells were sorted via flow cytometry and maintained as a polyclonal pool of 293T-ACE2 cells in DMEM containing 10% heat-inactivated FBS (vol/vol), 10mM HEPES, 1mM sodium pyruvate, and 100 U ml^{-1} penicillin/streptomycin at 37°C in 5% CO_2.

Viruses

To generate HIV-1 based SARS pseudotyped viral stocks, HEK293T cells were co-transfected with CMV-Luc, RΔ8.2 backbone plasmid, pTMPRSS2 and pSARS-CoV-S_{trunc} or pSARS-CoV-2_{trunc} using polyethylenimine. Six hours post-transfection, cells were washed twice with RPMI and fresh media (10% DMEM) was added. Supernatants containing virions were harvested 48 hours post-transfection, filtered and stored at -80°C. infectivity of pseudoviruses was determined by titration on 293T-ACE2 cells.

Neutralization Assays

SARS-CoV and SARS-CoV-2 S protein were co-transfected with an HIV-1 backbone and helper plasmid expressing firefly luciferase and serine protease TMPRSS2 (CMV-Luc, RΔ8.2 backbone plasmid, pTMPRSS2) in 1.25 x 10^5 HEK293T cells for 48 hours. Post-transfection, culture supernatants were harvested, filtered and stored at -80^{o}C. For determination of neutralization potential of bnAbs, eight-point titration curves with 2-fold serial dilution starting at 10 µg/ml, were performed. Serially diluted bnAbs were mixed with pseudotyped viruses for 1 hour at 37^{o}C. pseudovirus/bnAb combinations were then added to 293T-ACE2 cells pre-seeded (24-hours) at 10,000 cells/well. After 48 – 72 hours, supernatant was removed and luminescence was measured on Tecan luminescence plate reader using Bright Glow reagent. The percent infectivity was calculated as ratio of relative luminescence units (RLU) readout in the presence of bnAbs normalized to RLU readout in the absence of mAb. The half maximal inhibitory concentrations (IC50) were determined using 4-parameter logistic regression (GraphPad Prism version 8.3).

Biolayer interferometry analysis of the SARS-CoV-2 RBD binding affinity with N6 bnAb

Biolayer interferometry was performed using an Octet Red96 instrument (ForteBio, Inc.). A 5 µg/ml concentration of SARS-CoV-2 RBD-His was immobilized on a Ni-NTA coated biosensor surface. The baseline was obtained by measurements taken for 30 s in running buffer (1x PBS, 0.1% BSA and 0.02% Tween-20), and then, the sensors were subjected to association phase immersion for 300 s in wells containing N6 bnAb diluted in running buffer. Then, the sensors were immersed in running buffer for 600 s to measure dissociation. Biosensor was then regenerated by dipping it in EDTA followed by nickel sulfate solution. The mean Kon, Koff and apparent KD values of the SARS-CoV-2 RBD binding affinity for N6 bnAb were calculated from all the binding curves based on their global fit to a 1:1 Langmuir binding model.

Cell surface binding assay

1.25 x 10^5 HEK293T cells seeded in a 12-well plate were transiently transfected with 1.25 µg of SARS-CoV-2 S full-length protein using PEI-MAX. 48 hours post-transfection, cells were harvested and per experimental requirement, distributed in 1.5 ml microcentrifuge tubes. For monoclonal antibody staining, 10 µg/ml of antibody was used and titrated 2-fold in staining buffer. 100 µl of primary antibody (HIV-1 specific monoclonals) were added to HEK293T cells expressing SARS-CoV-2 S, and incubated for 30 minutes at room temperature. After washing, 100 µl of 1:500 diluted PE conjugated mouse anti-human IgG Fc was added, and after 30-minute incubation, a total of 50,000 cells were acquired on BD LSRFortessa X20. Data was analyzed using FlowJo software (version v10.6.1).

Statistics and Reproducibility

All statistical analyses were performed on GraphPad Prism 8.3. A p-value of <0.05 was considered significant. Neutralization assays were performed in triplicates and repeated thrice. Average IC50 values are shown and used for statistical comparisons. Binding ELISAs were performed in duplicates and repeated thrice. Average OD_{450} values were used for plotting curves. Surface binding assay was

281 performed thrice and average PE-MFI (phycoerythrin-median fluorescence intensity) values were used
282 for plotting curves.

283 **Acknowledgements**

284 We are grateful to Dr. Raiees Andrabi for providing the $S2P_{ecto}$ and RBD constructs for SARS-CoV and
285 SARS-CoV-2, and Dr. Paul Bieniasz for providing the full-length envelope constructs of SARS-CoV,
286 SARS-CoV-2 and pNL4-3ΔEnv-nanoluc. We are thankful to NIH AIDS Reagent program for providing
287 HIV-1 envelope pseudovirus plasmids, bnAbs, non-nAbs and their expression plasmids, and TZM-bl
288 cells, and Neutralizing Antibody Consortium (NAC), IAVI, USA for providing bnAbs. We are thankful to
289 Dr. Michel Nussenzweig for providing 10-1074 and BG18 bnAb expression plasmids.

290 **Author contributions**

291 N.M conceived and designed the study, performed binding ELISA, neutralization assay, analyzed data,
292 wrote the initial manuscript, revised and finalized the manuscript. Sd.S. and S.K purified and expressed
293 monoclonal antibodies. N.M and S.S expressed and purified recombinant proteins. T.B and N.J
294 performed binding ELISA. S.K edited and revised the manuscript. R.A.M, S.S and K.L conceived and
295 designed the study. K.L conceptualized and designed the study, edited, revised and finalized the
296 manuscript.

297 **Funding**

298 This work was supported in part by Science and Engineering Research Board (SERB), Department of
299 Science and Technology (DST), India (EMR/2015/001276) and Department of Biotechnology (DBT),
300 India (BT/PR5066/MED/1582/2012).

301 **Competing interests**

302 The authors declare no competing interests.

303 **Data Availability**

304 All data required to state the conclusions in the paper are present in the paper and/or the supplementary
305 data. Source data are provided with this paper. Additional information related to the paper, if required,
306 can be requested from the authors.

307 **References**

308 1. Walker LM, Burton DR. 2018. Passive immunotherapy of viral infections: “super-antibodies”
309 enter the fray. Nat Rev Immunol 18:297–308.

310 2. Kwong PD, Mascola JR. 2018. HIV-1 Vaccines Based on Antibody Identification, B Cell
311 Ontogeny, and Epitope Structure. Immunity 48:855–871.

312 3. Sok D, Burton DR. 2018. Recent progress in broadly neutralizing antibodies to HIV. Nat
313 Immunol 19:1179–1188.

314 4. Morgand M, Bouvin-Pley M, Plantier J-C, Moreau A, Alessandri E, Simon F, Pace CS, Pancera
315 M, Ho DD, Poignard P, Bjorkman PJ, Mouquet H, Nussenzweig MC, Kwong PD, Baty D,
316 Chames P, Braibant M, Barin F. 2016. V1/V2 Neutralizing Epitope is Conserved in Divergent
317 Non-M Groups of HIV-1. J Acquir Immune Defic Syndr 71:237–245.

318 5. Decaro N, Lorusso A. 2020. Novel human coronavirus (SARS-CoV-2): A lesson from animal
319 coronaviruses. Vet Microbiol 244:108693.

320 6. Hoffmann M, Kleine-Weber H, Schroeder S, Krüger N, Herrler T, Erichsen S, Schiergens TS,
321 Herrler G, Wu N-H, Nitsche A, Müller MA, Drosten C, Pöhlmann S. 2020. SARS-CoV-2 Cell
322 Entry Depends on ACE2 and TMPRSS2 and Is Blocked by a Clinically Proven Protease
323 Inhibitor. Cell 181:271-280.e8.

324 7. Wrapp D, Wang N, Corbett KS, Goldsmith JA, Hsieh C-L, Abiona O, Graham BS, McLellan JS.
325 2020. Cryo-EM structure of the 2019-nCoV spike in the prefusion conformation. Science
326 367:1260–1263.

327 8. Impagliazzo A, Milder F, Kuipers H, Wagner MV, Zhu X, Hoffman RMB, van Meersbergen R,
328 Huizingh J, Wanningen P, Verspuij J, de Man M, Ding Z, Apetri A, Kükrer B, Sneekes-Vriese E,
329 Tomkiewicz D, Laursen NS, Lee PS, Zakrzewska A, Dekking L, Tolboom J, Tettero L, van
330 Meerten S, Yu W, Koudstaal W, Goudsmit J, Ward AB, Meijberg W, Wilson IA, Radošević K.
331 2015. A stable trimeric influenza hemagglutinin stem as a broadly protective immunogen.
332 Science 349:1301–1306.

333 9. Watanabe Y, Allen JD, Wrapp D, McLellan JS, Crispin M. 2020. Site-specific glycan analysis of
334 the SARS-CoV-2 spike. Science 369:330–333.

335 10. Pinto D, Park Y-J, Beltramello M, Walls AC, Tortorici MA, Bianchi S, Jaconi S, Culap K, Zatta F,
336 De Marco A, Peter A, Guarino B, Spreafico R, Cameroni E, Case JB, Chen RE, Havenar-
337 Daughton C, Snell G, Telenti A, Virgin HW, Lanzavecchia A, Diamond MS, Fink K, Veesler D,

Corti D. 2020. Cross-neutralization of SARS-CoV-2 by a human monoclonal SARS-CoV antibody. Nature 583:290–295.

11. Zhou T, Zheng A, Baxa U, Chuang G-Y, Georgiev IS, Kong R, O'Dell S, Shahzad-Ul-Hussan S, Shen C-H, Tsybovsky Y, Bailer RT, Gift SK, Louder MK, McKee K, Rawi R, Stevenson CH, Stewart-Jones GBE, Taft JD, Waltari E, Yang Y, Zhang B, Shivatare SS, Shivatare VS, Lee C-CD, Wu C-Y, NISC Comparative Sequencing Program, Mullikin JC, Bewley CA, Burton DR, Polonis VR, Shapiro L, Wong C-H, Mascola JR, Kwong PD, Wu X. 2018. A Neutralizing Antibody Recognizing Primarily N-Linked Glycan Targets the Silent Face of the HIV Envelope. Immunity 48:500-513.e6.

12. Gristick HB, von Boehmer L, West AP, Schamber M, Gazumyan A, Golijanin J, Seaman MS, Fätkenheuer G, Klein F, Nussenzweig MC, Bjorkman PJ. 2016. Natively glycosylated HIV-1 Env structure reveals new mode for antibody recognition of the CD4-binding site. Nat Struct Mol Biol 23:906–915.

13. Wagh K, Kreider EF, Li Y, Barbian HJ, Learn GH, Giorgi E, Hraber PT, Decker TG, Smith AG, Gondim MV, Gillis L, Wandzilak J, Chuang G-Y, Rawi R, Cai F, Pellegrino P, Williams I, Overbaugh J, Gao F, Kwong PD, Haynes BF, Shaw GM, Borrow P, Seaman MS, Hahn BH, Korber B. 2018. Completeness of HIV-1 Envelope Glycan Shield at Transmission Determines Neutralization Breadth. Cell Rep 25:893-908.e7.

14. Seabright GE, Cottrell CA, van Gils MJ, D'addabbo A, Harvey DJ, Behrens A-J, Allen JD, Watanabe Y, Scaringi N, Polveroni TM, Maker A, Vasiljevic S, de Val N, Sanders RW, Ward AB, Crispin M. 2020. Networks of HIV-1 Envelope Glycans Maintain Antibody Epitopes in the Face of Glycan Additions and Deletions. Structure 28:897-909.e6.

15. ter Meulen J, van den Brink EN, Poon LLM, Marissen WE, Leung CSW, Cox F, Cheung CY, Bakker AQ, Bogaards JA, van Deventer E, Preiser W, Doerr HW, Chow VT, de Kruif J, Peiris JSM, Goudsmit J. 2006. Human monoclonal antibody combination against SARS coronavirus: synergy and coverage of escape mutants. PLoS Med 3:e237.

16. Rudicell RS, Kwon YD, Ko S-Y, Pegu A, Louder MK, Georgiev IS, Wu X, Zhu J, Boyington JC, Chen X, Shi W, Yang Z-Y, Doria-Rose NA, McKee K, O'Dell S, Schmidt SD, Chuang G-Y, Druz A, Soto C, Yang Y, Zhang B, Zhou T, Todd J-P, Lloyd KE, Eudailey J, Roberts KE, Donald BR, Bailer RT, Ledgerwood J, NISC Comparative Sequencing Program, Mullikin JC, Shapiro L, Koup RA, Graham BS, Nason MC, Connors M, Haynes BF, Rao SS, Roederer M, Kwong PD, Mascola JR, Nabel GJ. 2014. Enhanced potency of a broadly neutralizing HIV-1 antibody in vitro improves protection against lentiviral infection in vivo. J Virol 88:12669–12682.

17. Huang J, Kang BH, Ishida E, Zhou T, Griesman T, Sheng Z, Wu F, Doria-Rose NA, Zhang B, McKee K, O'Dell S, Chuang G-Y, Druz A, Georgiev IS, Schramm CA, Zheng A, Joyce MG, Asokan M, Ransier A, Darko S, Migueles SA, Bailer RT, Louder MK, Alam SM, Parks R, Kelsoe G, Von Holle T, Haynes BF, Douek DC, Hirsch V, Seaman MS, Shapiro L, Mascola JR, Kwong PD, Connors M. 2016. Identification of a CD4-Binding-Site Antibody to HIV that Evolved Near-Pan Neutralization Breadth. Immunity 45:1108–1121.

18. Makhdoomi MA, Khan L, Kumar S, Aggarwal H, Singh R, Lodha R, Singla M, Das BK, Kabra SK, Luthra K. 2017. Evolution of cross-neutralizing antibodies and mapping epitope specificity in plasma of chronic HIV-1-infected antiretroviral therapy-naïve children from India. J Gen Virol 98:1879–1891.

19. Kumar S, Panda H, Makhdoomi MA, Mishra N, Safdari HA, Chawla H, Aggarwal H, Reddy ES, Lodha R, Kumar Kabra S, Chandele A, Dutta S, Luthra K. 2018. An HIV-1 broadly neutralizing antibody from a clade C infected pediatric elite neutralizer potently neutralizes the contemporaneous and autologous evolving viruses. J Virol https://doi.org/10.1128/JVI.01495-18.

20. Mishra N, Makhdoomi MA, Sharma S, Kumar S, Dobhal A, Kumar D, Chawla H, Singh R, Kanga U, Das BK, Lodha R, Kabra SK, Luthra K. 2019. Viral Characteristics Associated with Maintenance of Elite Neutralizing Activity in Chronically HIV-1 Clade C-Infected Monozygotic Pediatric Twins. J Virol 93.

21. Corti D, Misasi J, Mulangu S, Stanley DA, Kanekiyo M, Wollen S, Ploquin A, Doria-Rose NA, Staupe RP, Bailey M, Shi W, Choe M, Marcus H, Thompson EA, Cagigi A, Silacci C, Fernandez-Rodriguez B, Perez L, Sallusto F, Vanzetta F, Agatic G, Cameroni E, Kisalu N,

Gordon I, Ledgerwood JE, Mascola JR, Graham BS, Muyembe-Tamfun J-J, Trefry JC, Lanzavecchia A, Sullivan NJ. 2016. Protective monotherapy against lethal Ebola virus infection by a potently neutralizing antibody. Science 351:1339–1342.

22. Corti D, Zhao J, Pedotti M, Simonelli L, Agnihothram S, Fett C, Fernandez-Rodriguez B, Foglierini M, Agatic G, Vanzetta F, Gopal R, Langrish CJ, Barrett NA, Sallusto F, Baric RS, Varani L, Zambon M, Perlman S, Lanzavecchia A. 2015. Prophylactic and postexposure efficacy of a potent human monoclonal antibody against MERS coronavirus. Proc Natl Acad Sci USA 112:10473–10478.

23. Levine MM. 2019. Monoclonal Antibody Therapy for Ebola Virus Disease. N Engl J Med 381:2365–2366.

24. Barnes CO, West AP, Huey-Tubman KE, Hoffmann MAG, Sharaf NG, Hoffman PR, Koranda N, Gristick HB, Gaebler C, Muecksch F, Lorenzi JCC, Finkin S, Hägglöf T, Hurley A, Millard KG, Weisblum Y, Schmidt F, Hatziioannou T, Bieniasz PD, Caskey M, Robbiani DF, Nussenzweig MC, Bjorkman PJ. 2020. Structures of Human Antibodies Bound to SARS-CoV-2 Spike Reveal Common Epitopes and Recurrent Features of Antibodies. Cell 182:828-842.e16.

25. Liu L, Wang P, Nair MS, Yu J, Rapp M, Wang Q, Luo Y, Chan JF-W, Sahi V, Figueroa A, Guo XV, Cerutti G, Bimela J, Gorman J, Zhou T, Chen Z, Yuen K-Y, Kwong PD, Sodroski JG, Yin MT, Sheng Z, Huang Y, Shapiro L, Ho DD. 2020. Potent neutralizing antibodies against multiple epitopes on SARS-CoV-2 spike. Nature 584:450–456.

26. Wang C, Li W, Drabek D, Okba NMA, van Haperen R, Osterhaus ADME, van Kuppeveld FJM, Haagmans BL, Grosveld F, Bosch B-J. 2020. A human monoclonal antibody blocking SARS-CoV-2 infection. Nat Commun 11:2251.

27. Zost SJ, Gilchuk P, Case JB, Binshtein E, Chen RE, Nkolola JP, Schäfer A, Reidy JX, Trivette A, Nargi RS, Sutton RE, Suryadevara N, Martinez DR, Williamson LE, Chen EC, Jones T, Day S, Myers L, Hassan AO, Kafai NM, Winkler ES, Fox JM, Shrihari S, Mueller BK, Meiler J, Chandrashekar A, Mercado NB, Steinhardt JJ, Ren K, Loo Y-M, Kallewaard NL, McCune BT, Keeler SP, Holtzman MJ, Barouch DH, Gralinski LE, Baric RS, Thackray LB, Diamond MS,

Carnahan RH, Crowe JE. 2020. Potently neutralizing and protective human antibodies against SARS-CoV-2. Nature 584:443–449.

28. Rogers TF, Zhao F, Huang D, Beutler N, Burns A, He W-T, Limbo O, Smith C, Song G, Woehl J, Yang L, Abbott RK, Callaghan S, Garcia E, Hurtado J, Parren M, Peng L, Ramirez S, Ricketts J, Ricciardi MJ, Rawlings SA, Wu NC, Yuan M, Smith DM, Nemazee D, Teijaro JR, Voss JE, Wilson IA, Andrabi R, Briney B, Landais E, Sok D, Jardine JG, Burton DR. 2020. Isolation of potent SARS-CoV-2 neutralizing antibodies and protection from disease in a small animal model. Science 369:956–963.

29. Malherbe DC, Wibmer CK, Nonyane M, Reed J, Sather DN, Spencer DA, Schuman JT, Guo B, Pandey S, Robins H, Park B, Fuller DH, Sacha JB, Moore PL, Hessell AJ, Haigwood NL. 2020. Rapid Induction of Multifunctional Antibodies in Rabbits and Macaques by Clade C HIV-1 CAP257 Envelopes Circulating During Epitope-Specific Neutralization Breadth Development. Front Immunol 11:984.

30. Hessell AJ, Malherbe DC, Pissani F, McBurney S, Krebs SJ, Gomes M, Pandey S, Sutton WF, Burwitz BJ, Gray M, Robins H, Park BS, Sacha JB, LaBranche CC, Fuller DH, Montefiori DC, Stamatatos L, Sather DN, Haigwood NL. 2016. Achieving Potent Autologous Neutralizing Antibody Responses against Tier 2 HIV-1 Viruses by Strategic Selection of Envelope Immunogens. J Immunol 196:3064–3078.

31. Jones AT, Chamcha V, Kesavardhana S, Shen X, Beaumont D, Das R, Wyatt LS, LaBranche CC, Stanfield-Oakley S, Ferrari G, Montefiori DC, Moss B, Tomaras GD, Varadarajan R, Amara RR. 2018. A Trimeric HIV-1 Envelope gp120 Immunogen Induces Potent and Broad Anti-V1V2 Loop Antibodies against HIV-1 in Rabbits and Rhesus Macaques. J Virol 92.

32. Havenar-Daughton C, Sarkar A, Kulp DW, Toy L, Hu X, Deresa I, Kalyuzhniy O, Kaushik K, Upadhyay AA, Menis S, Landais E, Cao L, Diedrich JK, Kumar S, Schiffner T, Reiss SM, Seumois G, Yates JR, Paulson JC, Bosinger SE, Wilson IA, Schief WR, Crotty S. 2018. The human naive B cell repertoire contains distinct subclasses for a germline-targeting HIV-1 vaccine immunogen. Sci Transl Med 10.

446 33. Jardine JG, Kulp DW, Havenar-Daughton C, Sarkar A, Briney B, Sok D, Sesterhenn F, Ereño-
447 Orbea J, Kalyuzhniy O, Deresa I, Hu X, Spencer S, Jones M, Georgeson E, Adachi Y, Kubitz M,
448 deCamp AC, Julien J-P, Wilson IA, Burton DR, Crotty S, Schief WR. 2016. HIV-1 broadly
449 neutralizing antibody precursor B cells revealed by germline-targeting immunogen. Science
450 351:1458–1463.

451